

Construction of a sense of force feedback and vision for micro-objects: Recreate the response and a sense of force of objects

T.Domoto

Graduate School of Computer Science
and System Engineering
Kyushu Institute of Technology
680-4, Iizuka City, Fukuoka, Japan, 820-8502
dohmoto@mmcs.mse.kyutech.ac.jp

E. Hayashi

Department of Mechanical Information
Science and Technology
Kyushu Institute of Technology
680-4, Iizuka City, Fukuoka, Japan, 820-8502
haya@mse.kyutech.ac.jp

Abstract. The purpose of this research was to develop a combined sense system that uses both force feedback and visual feedback to determine the shape of the microscopic features of a microsample. Efficiency in performing minute procedures would be improved if the operator could have a sense of force while using a manipulator. We used a cantilever to touch a minute object and obtain a reaction force from the degree of bending. We constructed a haptic device that gives a sense of that force to the operator when touching the sample with a cantilever. When the haptic device was used in simulations, the user could feel a force as if he had touched the sample.

Key words: force feedback, haptic interface, simulation.

1. Introduction

Technologies that can accurately perform minute work are now being sought for medical treatment and in the field of manufacturing semiconductors. Such minute work is improved by using micromanipulators, but their operation is difficult because the operator has no sense of force; he or she relies only on sight through a microscope. As a result, a person skilled in the use of this technology is needed for all minute work. The efficiency of minute work would be improved if the operator were able to have a sense of force while using a manipulator.

Here we describe the development of a more efficient system for minute operations. Our aim was to develop a system using not only the sense of sight through a microscope but also a sense of force from the manipulator. For this fundamental research, a system was created to assess the reaction force when a minute sample was touched. A cantilever was used to touch the sample, and the reaction force was obtained from the degree to which the sample bent. In addition, we used a haptic device and amplified the force feedback from a minute sample of a virtual object.

2. System Structure

2-1. System summary

The system structure is shown in Fig. 1a, and a schematic view is shown in Fig. 1b. This system consists of a microscope with an automatic x-y stage, a piezo stage, a feedback stage controller to control the x-y stage, a piezo stage controller, a haptic device for transmitting force feedback (Fig. 2), a cantilever (Fig. 3), and a PC via which the user can control and operate these components. The sample was fixed on the x-y stage by an injector (Fig. 4) and a holding pipette (Fig. 5). When

the cantilever, which was fixed to the piezo stage, touched the sample, the operator could maintain the cantilever's position by obtaining the value of the reaction force through the interface. The resolution of the piezo stage is 1 nm.



Fig. 1a. Photograph of the system structure.

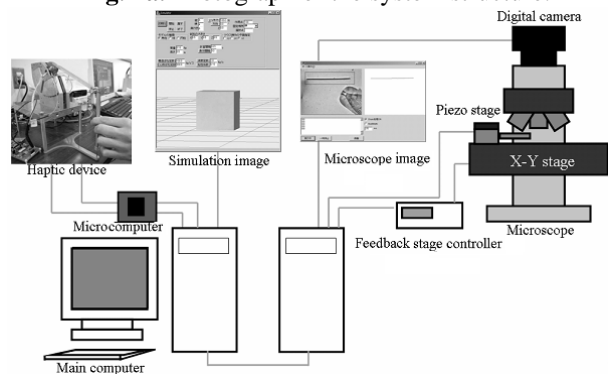


Fig. 1b. A schematic view of the system structure

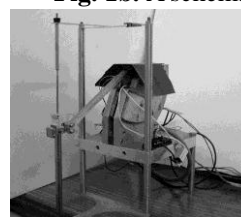


Fig. 2. Haptic device.

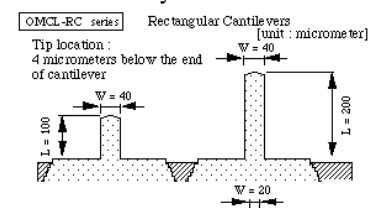


Fig. 3. Cantilever.



Fig. 4. Injector.

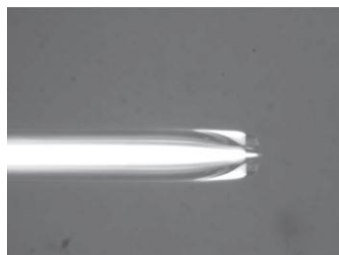


Fig. 5. Tip of holding pipette.

2-2. Haptic device

Figure 6 provides a diagram of the haptic device. It consists primarily of a rotor, a laser, and a position-sensitive device (PSD). We installed a coil on the rotor with a polarity magnet, which generated electromagnetic induction by an electric current and a magnetic force. The angle of the rotor can be measured by the laser and the PSD. The rotor was able to follow any input waveform.

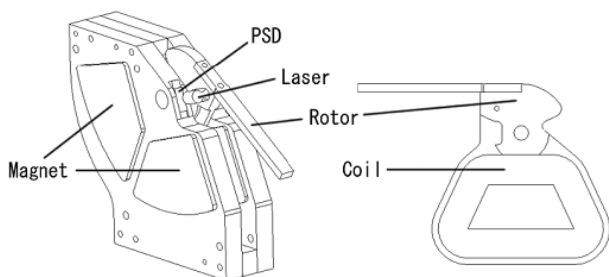


Fig. 6. Diagram of the haptic device.

The actuator is controlled by a servomechanism on the actuator. The system driving the actuator therefore consisted of four actuators: a microcomputer, an inputting AD/DA port, an outputting microcomputer, and a PC outputting order value. The system controls the actuator during each part of the process. Figure 7 shows the structure of the haptic device.

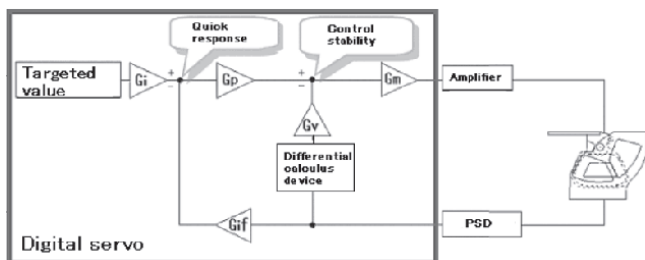


Fig. 7. Structure of the haptic device.

The actuator, whose actions are governed by the PD control, is operated through a digital differential calculus device. A transfer function for the quadratic function system shown in Fig. 8 is provided for the actuator servo system. The role of each parameter of the control system is to adjust the total offset to a master in G_i/G_{if} , to regulate the item viscosity/resonance point in G_p/G_v , and to regulate the total gain in G_m . Table 1 provides a list of the control parameters of the servomechanism system.

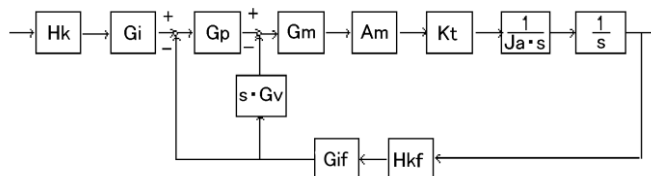


Fig. 8. Block diagram of the servomechanism system.

Table 1 Control parameters of the servomechanism system

Parameter	Reference	Unit
Hk	Position Voltage Constant	18.56 [V/rad]
Hkf	Position Voltage Feedback Constant	18.56 [V/rad]
Am	Amplifier Constant	0.8986 [A/V]
Kt	Torque Constant	0.6141 [Nm/A]
Ja	Moment of Inertia	0.000581 [kg·m]
Gi	Controller Input Gain	1
Gif	Position Feedback Gain	1
Gp	Position Gain	adjusted value
Gv	Velocity Gain	adjusted value
Gm	Manipulation Gain	1

3. Measuring the reaction force

The reaction force was used to calculate the force applied by the minute object. In this experiment, we touched the minute object with the cantilever shown in Fig. 3, and the reaction force was obtained based on the degree of bend of the cantilever. The layout of the experiment is shown in Figs. 7 and 8, and the environment of the experiment is shown in Figs. 9 and 10. Based on this experiment, we were able to determine the reaction force applied by the minute object.

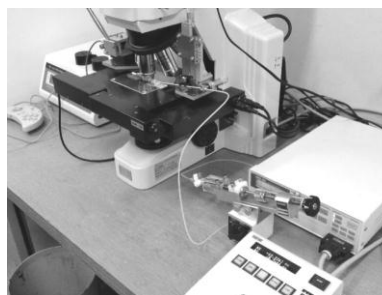


Fig. 9. Environment of the experiment.



Fig. 10. Close-up of the environment of the experiment.

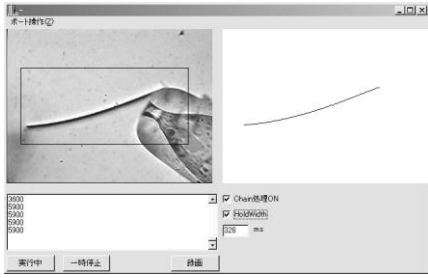


Fig. 11. Cantilever touching the tip of the holding pipette.

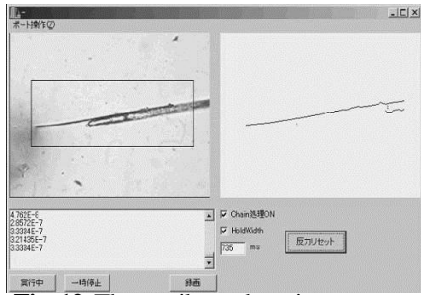


Fig. 12. The cantilever detection program.

Figure 11 shows the cantilever touching the tip of the holding pipette. Figure 12 shows the experiment that measures the reaction force of the downy hair. The image-processing speed of the cantilever was improved by the tracking process. The bend of the cantilever is assumed to be linear-elastic so that Hooke's law may be applied. The restoring force, F , of the bend of the cantilever is given by

$$F = kx \quad (1)$$

where x is the compression distance from the equilibrium position, and k is the spring constant.

4. Deforming the sample in simulation

In this study, we attempted to build a working system using a microscope, a haptic device, and a simulation. A fundamental element was simulating the deformation of a minute object. Figure 13 shows the graphical user interface (GUI) of the simulator. A graphic tool was created using OpenGL to draw the object and to choose the shape of the sample, for instance, a cube or sphere. The dynamic model of the sample consisted of a spring-mass array of mass points in both the vertical and horizontal directions. An example of the arrangement of mass points is shown in Fig. 14. When a force was applied at a mass point, the simulation calculated the speed of all mass points that had been affected. The image was renewed after every ten calculations.

We defined a spring as having a size but no weight, and a mass point as having a size, a weight, and a rigid body. An arbitrary mass object can be placed on a spring on a bitmap (Fig. 15). In addition, a sample can be seen from various viewpoints, and the deformation of the sample, which is impossible to observe by microscope, can be checked. The shape of this object can be either a cube or a sphere, and any

point may be selected as a fixed point or an operating point.

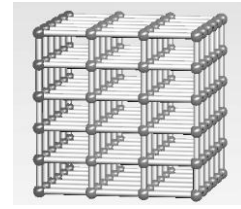
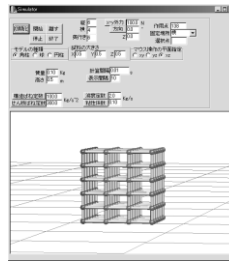


Fig. 13. Simulator.

Fig. 14. Arrangement of mass points

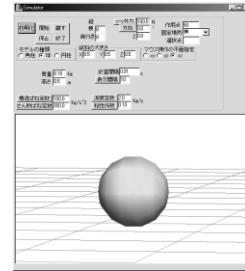


Fig. 15. Placing an arbitrary object on a bitmap.

The calculation method for the displacement of each mass point is based on Newton's equation of motion (Eq. 1) using the Euler method. A mass point is linked to an adjacent mass point at both ends of a spring. When the spring between the mass points is in the equilibrium position, the restoring force, F , is the sum of the elastic force of the construction spring and the shear spring, and the viscous force is given by

$$ma = \sum F \quad (2)$$

where m is mass and a is acceleration.

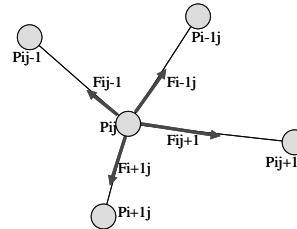


Fig. 16. Elasticity.

$\sum F$ is the sum of the elastic force of the construction spring and shear spring, the viscous force, and the damping force. To obtain F , we divided the restoring force into $F_{damping}$, F_{spring} , and $F_{viscous}$. Equation 2 gives the following equations using the model shown in Fig. 16:

$$F_{spring} = \sum F_{ij} \quad (3)$$

$$F_{damping} = -C_d v_i \quad (4)$$

$$F_{viscous} = -C_v (v_i - v_j) \quad (5)$$

$$\sum F = F_{spring} + F_{damping} + F_{viscous} \quad (6)$$

where C_d is the damping factor, C_v is viscosity, and v_i and v_j are the velocities.

5. Characteristic measurements and a reappearance experiment for an object

Dynamic and static characteristics of the object were measured and then recreated using the haptic device. The object used this time was silicon manufactured by KYOUTOKAGAKU. The silicon sheet thickness was 2 or 3 [mm]. Each characteristic when silicon was stacked up was measured. Figure17 shows the response of the silicon and the response of the haptic device. Figure18 shows the reaction force of the silicon and the output power of the haptic device.

In the last program, parameters cannot be changed during operation. However, the response of the silicon used for the experiment in this case was could not recreate one parameter, and the sense of force was not linear. Therefore, the program was implemented so that parameters could be changed during operation.

Table 2 shows the frequency, constant of spring, and damping coefficient in each ectopic focus when the dynamic characteristic is recreated. Table 3 shows the frequency and constant of spring in each ectopic focus when the static characteristic is recreated.

The characteristics recreated by the haptic device, and the experiment was evaluated. In this experiment, there was a tendency for a touch feeling close to that of real silicon to be created when the static characteristic was recreated.

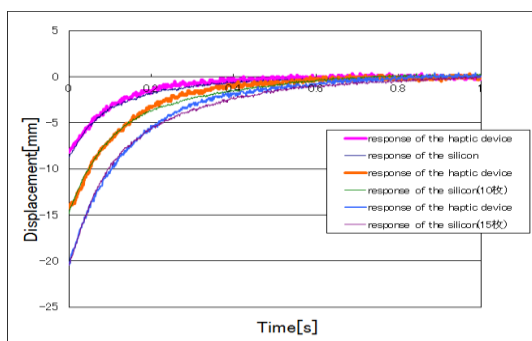


Fig. 17. Unit step response

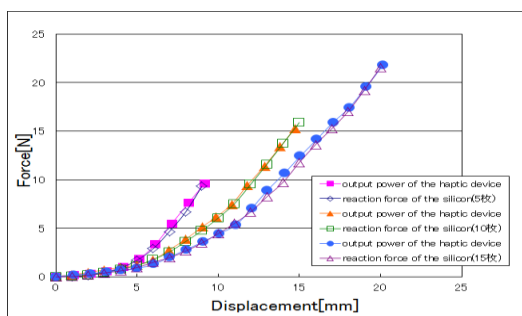


Fig. 18. Displacement_Force related diagram

Table 2. Haptic device parameter with a dynamic characteristic

Displacement[mm]	5 sheet			10 sheet			15 sheet		
	frequency[Hz]	constant of spring[N/mm]	damping coefficient	frequency[Hz]	constant of spring[N/mm]	damping coefficient	frequency[Hz]	constant of spring[N/mm]	damping coefficient
0									
1	4.5	0.0272	1.6	4.2	0.0205	1.7			
2									
3	4.5	0.0272	1.7				4	0.0174	1.7
4									
5				4.2	0.0205	1.8			
6	4.5	0.0272	1.4						
7									
8									
9									
10									
11				4.2	0.0205	1.3			
12							4	0.0174	1.8
13									
14									
15									
16									
17									
18									
19							4	0.0174	1.4
20									

Table 3. Haptic device parameter with a static characteristic

Displacement[mm]	5 sheet		10 sheet		15 sheet	
	frequency[Hz]	constant of spring[N/mm]	frequency[Hz]	constant of spring[N/mm]	frequency[Hz]	constant of spring[N/mm]
0						
1						
2	9.4	0.175	10.6	0.220		
3					9.4	0.175
4						
5						
6	20	0.782				
7						
8						
9			22.5	1.01		
10	30	1.95			20	0.782
11						
12						
13			30	1.95		
14						
15						
16						
17						
18						
19					30	1.95
20						

6. Conclusion

In the present study the characteristics of silicon were measured and recreated, and evaluations were carried out with regard to response and sense of force using a haptic device. The touch judging program of the haptic device and sample simulation was implemented. It was found that the spring constants differed greatly with regard to both dynamic and static characteristics in this experiment. The characteristics of various objects will be measured in the future, and The characteristics recreated

Future research should focus on building a system that allows a reaction force to be detected and shown more precisely. Such a system would make it possible to test smaller samples.

7. Acknowledgement

This research was partially supported by the Ministry of Education, Science, Sports and Culture, Grant-in-Aid for Scientific Research, 2011.

References

1. Noda R (2011) Construction of super-micro sense of force feedback and visual for micro objects. Kyushu Institute of Technology. Proceedings of the 15th International Symposium on Artificial Life and Robotics, Beppu, Oita, Japan, 2011